

Modeling Interface Response in Cellular Adhesion

G. Megali^{*1}, D. Pellicanò¹, M. Cacciola¹, F. Calarco¹, D. De Carlo¹, F. Laganà¹ and F. C. Morabito¹
¹DIMET Department, University “Mediterranea” of Reggio Calabria, Via Graziella Feo di Vito, I-89100 Reggio Calabria (Italy)

*Corresponding author: postal address: Via Graziella Feo di Vito I-89100 Reggio Calabria (Italy),
 email address: giuseppe.megali@unirc.it

Abstract: Constitutive properties of living cells are able to withstand physiological environment as well as mechanical stimuli occurring within and outside the body. In this context, a quantitative study in single cell mechanics needs to be conducted. Particularly, we will examine fluid flow and Neo-Hookean deformation related to the rolling effect. A mechanical model to describe the cellular adhesion with detachment is here proposed. We develop a Finite Element analysis, simulating blood cells attached on vessel wall. Restricting the interest on the contact surface and elaborating again the computational results, we develop an equivalent spring model. The simulation notices deformation inhomogeneities (i.e. areas with different concentrations having different deformation values). This important observation should be connected with a specific form of the stored energy deformation. In this case, it loses the standard convexity to show a non-monotone deformation law. Consequently, we have more minimum and the variational problem seems more difficult.

Keywords: Cell detachment, Rolling effect, Contact with adhesion, Fluid-structure interaction, Finite Element Method.

1. Introduction

In order to physically model and determine the effect of the blood flow in presence of a human cell, a Finite Element Method (FEM)-based approach has been exploited. It requires the geometrical and physical definition of the blood vessel, the cell and flow parameters. For our purpose, we verify cell deformation under actual conditions (see Figure 1 [1] and 2). Thus, a brief description of the theoretical framework for the mechanical is given. Then, we describe the exploited approach through FEM analysis simulating the human cell and the blood flow, and so modeling an endothelial wall cross of a blood flow.

Our aim was to focus the contact part among cell and endothelial wall about the deformation field. Our opinion is that the simulation notice the deformation inhomogeneity namely different concentration areas with different deformation values. This important observation should be connected with a specific form of the stored energy deformation that, in this case, loses the standard convexity to show the multi-well form. Consequently, we have more minimum and the variational problem seems more difficulty.

Solutions through minimizing sequence are applied and this relieve microstructure formation.

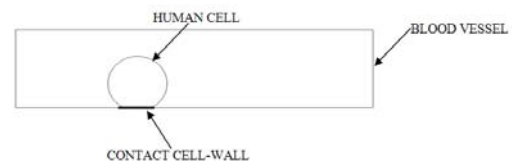


Figure 1. Geometrical representation of the model

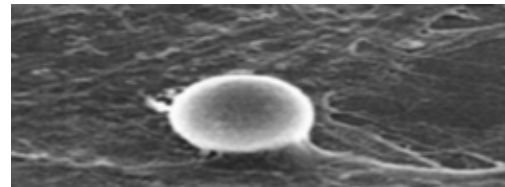


Figure 2. 3D-view of cell deformation in a real image in presence of blood flow

2. The Rolling Effect

Rolling effect [2] is a particular case of cell adhesion and it involves several phenomena of diverse nature: mechanical, physical or chemical interactions. One of the most important point concerns the adhesion molecules lying on the surface of the cell and on the wall, characterized by their chemical properties and density. The creation of connections between the cell and the wall can occur if the molecules being present, the ligands (on the cell) and the receptors (on the wall) respectively, are sufficiently close to each other, and if the chemical affinity is strong

enough [3]. The rolling of the cell consists in the simultaneous creation and rupture of connections when the system is subjected to a fluid flow. The most important example in this case is the slowing down of the leukocyte cell during the immune defense (see Figure 3). In the general case, the interface zone involves free adhesion molecules: ligands, receptors and connections, which represent the junction between the ligands of the wall and the receptors of the cell [4]. The cell membrane stiffness increases, in the case of an adhering cell, because of the local reinforcement of the cytoskeleton: this is due to the presence of external chemiotactic particles, which create an external signal [3, 5].

3. Theoretical Framework

3.1 Mechanical Aspects

The From mechanical point of view this is a detachment problem and, according to Villaggio [6], Leitman and Villaggio [7], it can be formulated as the peeling of an adhesive membrane initially glued to a flat surface. Regarding the cell as membrane solid pulled with a forces system, we say that, when the blood flow is regular the cell will remain perfectly glued to the endothelial wall, while when the flow intensity augments part of cell may be pulled away. Let u the displacement field, then the equation of motion hold

$$\rho \frac{\partial^2 \mathbf{u}}{\partial t^2} + T \nabla^2 \mathbf{u} = f(x, y, t) \text{ on } \Omega \quad (1)$$

where ρ is the supposed constant density and T the stress tensor. Clearly a the boundary of the detached part we have

$$u = 0 \text{ on } \Omega D \quad (2)$$

Here the problem is the determination of ΩD . By Villaggio [1] we recall the breaking condition in the form

$$(T - \rho v^2) \partial u / \partial n = -F \text{ on } \Omega D \quad (3)$$

where v denotes the normal velocities of ΩD , $\partial u / \partial n$ is the normal outer of u on ΩD and F is the cohesive forces. The closed form of (1) exists only for some particular cases. For instance let f^* the static resultant of the flow actions and supposing it just applied at the origin of the system. So, in this case $f(x, y, t) = f^* \delta(x) \delta(y)$ with

$\delta(\cdot)$ the delta function. For instance supposing the u filed symmetrical about to the origin, we consider a circular region and so $u = u(r)$ and the region ΩD becomes a circular region which radius is λ . Under this consideration the solution of (1) has the form

$$u(r) = (f^*/2\pi T) \ln r + \cos(t) \quad (4)$$

namely

$$u(r) = (f^*/2\pi T) \ln(r/\lambda) \quad (5)$$

and in $v = 0$

$$\lambda = (f^*/2\pi F) \quad (6)$$

The complete solution in closed form becomes

$$u(r) = (f^*/2\pi F) \ln(2\pi fr / f^*) \text{ on } r \leq \lambda \quad (7)$$

3.2 FEM Model Generation

In this section of the paper we show how to simulate the effect of a blood flow in presence of a cell in a blood vessel. Using our FEM package [8-10], the blood flow and pressure drop across human cell have been studied and a mathematical model of the process has been constructed and analyzed. The constructed mathematical model consists of the equations of continuity (representing conservation of mass), motion (representing conservation of momentum) for the flow of blood through human cell [11] (see Figure 4 [12]).

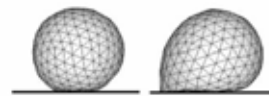


Figure 3. 2D-view of cell deformation effect: at $t_0=0$ (s) on the left and at $t_1=0.125$ (s) on the right.

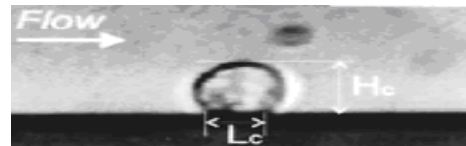


Figure 4. Schematic diagram of the side-view flow and cell adhesion. The fluid flows from left to right ($L_c=1$ (μm), $H_c=2.3$ (μm))

These equations are supplemented by appropriate models which represent the stress/strain behaviour of human cell [13].

Simulation of fluid-structure interaction is a challenging problem for computer modellers. Fluid flow and Neo-Hookean hyperelastic deformation modelling has been the subject of numerous research during the past few decades.

Our approach provides reliable simulations for both these steps. The study of these problems requires quantitative information regarding the interaction between blood flow and human cell deformation under realistic physiological conditions. The complexity of such a task is such that only computer based numerical simulations can be used. In this work we exploited FEM to solve the developed mathematical 2D model representing the operations of human cell. For our aims, the Comsol Multiphysics® package has been exploited. Computer modeling can help in this context if it is based on an appropriate mathematical model and an accurate reliable solution. So it is needed to fit a model to the problem and get a satisfactory solution.

3.3 Governing equation of elastic-solid deformation

For a purely elastic solid [10]:

$$\frac{\partial}{\partial x_j} \sigma_{ij} + f = 0 \quad (8)$$

$$\sigma_{ij} = -p\delta_{ij} + p_{ij} \quad (9)$$

σ is the strain tensor. Let \mathbf{u} is the displacement field, then under the material incompressible hypothesis

$$\nabla \cdot \mathbf{u} = 0 \quad (10)$$

$$\tau_{ij} = 2Ge_{ij} \quad (11)$$

$$p = -k(\nabla \cdot \mathbf{u}) \quad (12)$$

where G and k are, respectively, the shear modulus and the bulk modulus. Specific finite element techniques such as the penalty method are well suited to combine the described set of Neo-Hookean hyperelastic and fluid equations.

3.4 Governing equation fluid motion, conservation of mass and momentum

If an inelastic generalized Newtonian flow behavior is assumed [11, 12], the Cauchy stress tensor σ can be written as

$$\sigma = -p\mathbf{I} + 2\eta(\gamma)D_v \quad (13)$$

where $\eta(\gamma)$ is the shear-rate-dependent dynamic viscosity and D_v denotes the rate of deformation tensor

$$D_v = \frac{1}{2}[\nabla \mathbf{v} + (\nabla \mathbf{v})^T] \quad (14)$$

The shear rate parameter γ must be defined in terms of the second invariant of the rate of deformation tensor. For incompressible fluid this is

$$\gamma = \sqrt{2D_v : D_v} \quad (15)$$

The Non-Newtonian behavior of blood can be described very well with the Carreau-Yasuda model

$$\frac{\eta(\gamma) - \eta_\infty}{\eta_0 - \eta_\infty} = [1 + (\lambda\gamma)^a]^{\frac{n-1}{a}} \quad (16)$$

with η_0 , η_∞ , λ , a and n being parameters of the model. For a time constant $\lambda=0$ this model reduces to a simple Newtonian model with $\eta(\gamma)=\eta_0$.

4. COMSOL Mutiphysics Analysis

The following section shows proposed model for fluid-structure interactions. It illustrates how fluid flow can deform surrounding “structures” and how to solve for the flow in a continuously deforming geometry using the arbitrary Lagrangian-Eulerian technique [14-16]. The model geometry consists of a horizontal flow channel in the middle of which is a human cell, with a circular structure. The cell forces the fluid into a narrower path in the upper part of the channel, thus imposing a force on the structure’s walls resulting from the viscous drag and fluid pressure. The cell structure, being made of a Neo-Hookean hyperelastic material, bends under the applied load. Consequently, the fluid flow also follows a new path, so solving the flow in the original geometry would generate incorrect results. The Navier-Stokes equations that solve the flow are formulated for these moving coordinates. The simulations exploit the FEM and require geometrical and physical definition of the blood flow and the human cell [17]; the latter has been modeled as a circumference with a portion of perimeter adherent to the venous paries. In this example the flow channel is

100 (μm) high and 300 (μm) long. The cell structure has a radius of 1.25 (μm), and is adherent 1 (μm) long at the channel's bottom boundary. Assume that the structure is along the direction perpendicular to the image. The fluid is a water-like substance with a density $\rho=1000$ (kg/m^3) and dynamic viscosity $\eta=0.001$ ($\text{Pa}\cdot\text{s}$). To demonstrate the desired techniques, assume the cell structure consists of a Neo-Hookean hyperelastic material with a density $\rho=7850$ (kg/m^3) initial tangent $E=80$ (kPa). The model consists of a fluid part, solved with the Navier-Stokes equations in the flow channel, and a structural mechanics part, which you solve in the human cell. Transient effects are taken into account in both the fluid and the cell structure. The structural deformations are modeled using large deformations in the Plane Strain application mode. The displacements and displacement velocities are denoted u , v , u_s , and v_s , respectively. Fluid flow is described by the Navier-Stokes equations for the velocity field, $\mathbf{u}=(u,v)$, and the pressure, p , in the spatial (deformed) moving coordinate system:

$$\rho \frac{\partial \mathbf{u}}{\partial t} - \nabla \cdot [-\rho \mathbf{I} + \eta(\nabla \mathbf{u} + (\nabla \mathbf{u})^T)] + \rho(\mathbf{u} - \mathbf{u}_m) \cdot \nabla \mathbf{u} = \mathbf{F} \quad (17)$$

$$-\nabla \cdot \mathbf{u} = 0 \quad (18)$$

In these equations, \mathbf{I} denotes the unit diagonal matrix and \mathbf{F} is the volume force affecting the fluid. Assume that no gravitation or other volume forces affect the fluid, so that $\mathbf{F}=0$. The Navier-Stokes equations are solved in the spatial (deformed) coordinate system. At the inlet, the model uses a fully developed laminar flow. Zero pressure is applied at the outlet. No-slip boundary conditions, that is $\mathbf{u} = 0$, are used at all other boundaries. Note that this is a valid condition only as long as you are solving the stationary problem. In this transient version of the same model, with the cell starting out from an undeformed state, it is necessary to state that the fluid flow velocity be the same as the velocity of the deforming obstacle. The coordinate system velocity is $\mathbf{u}=(u_m, v_m)$. At the channel entrance on the left, the flow has fully developed laminar characteristics with a parabolic velocity profile (see Figure 5) but its amplitude changes with time.

At first, flow increases rapidly, reaching its peak value at 0.215 (s); thereafter it gradually decreases to a steady-state value of 3.33 (cm/s).

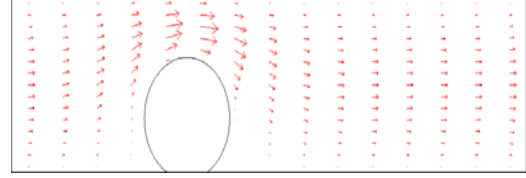


Figure 5. Schematic of the problem statement. Simulated flow with cell presence at $t=0.005$ (s).

The centerline velocity in the x direction, u_{in} , with the steady-state amplitude U comes from the equation

$$u_{in} = \frac{U \cdot t^2}{\sqrt{(0.04 - t^2)^2 + (0.1t)^2}} \quad (19)$$

where t must be expressed in seconds. At the outflow (right-hand boundary), the condition is $p=0$. On the solid (non deforming) walls, no-slip conditions are imposed, $u=0$, $v=0$, while on the deforming interface the velocities equal the deformation rate, $u_0=u_t$ and $v_0=v_t$. The structural deformations are solved for using an hyperelastic formulation and a nonlinear geometry formulation to allow large deformations. For boundary conditions, the cell is fixed to the bottom of the fluid channel, so that it cannot move in any direction. All other object boundaries experience a load from the fluid, given by

$$\mathbf{F}_T = -\mathbf{n} \cdot (-\rho \mathbf{I} + \eta(\nabla \mathbf{u} + (\nabla \mathbf{u})^T)) \quad (20)$$

where \mathbf{n} is the normal vector to the boundary. This load represents a sum of pressure and viscous forces. With deformations of this magnitude, the changes in the fluid flow domain have a visible effect on the flow and on the cell, too. Figure 6 shows the geometry deformation and flow at $t=4$ (s) when the system is close to its steady state.

Due to the channel's small dimensions, the Reynolds number (R) of the flow is small ($R \ll 100$), and the flow stays laminar in most of the area.

The swirls are restricted to a small area behind the structure.

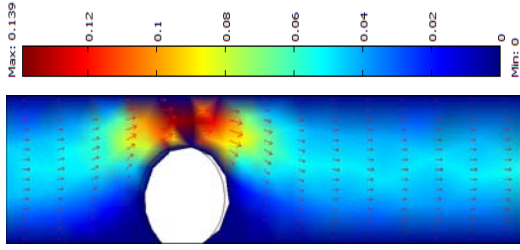


Figure 6. Simulated flow velocity and geometry deformation at $t=4$ (s). The vectors indicate the flow direction and the color scale indicates flow-velocity magnitude (m/s).

The amount of deformation as well as the size and location of the swirls depend on the magnitude of the inflow velocity. Most of time, the deformation follows the inflow velocity quite closely. Whenever the inflow velocity starts to decrease. Toward the end of the simulation, when inflow and structure deformation approach their steady-state values, the mesh velocity also decreases to zero. For the fluid domain are applied the following settings. For the boundary settings, we imposed a inlet condition with a mean velocity equal to u_{in} (set to 3.33 (cm/s)). For the sides we apply condition of wall with sliding absent; for the boundary ($\delta\Omega$) on the right we imposed type of outlet with a condition of pressure and no viscous stress with $p_0=0$. The edges of the cell are characterized by conditions wall mobile dispersant (structural displacement) with the exception of the base cell which is fixed and not involved in the dynamic physical process, according to

$$\mathbf{n}(\eta_1(\nabla\mathbf{u}_1 + (\nabla\mathbf{u}_1)^T) - \rho_1\mathbf{I} - \eta_2(\nabla\mathbf{u}_2 + (\nabla\mathbf{u}_2)^T) - \rho_2\mathbf{I}) = 0 \quad (21)$$

Our studies have been based on a discrete domain with 231 elements. The number of degree of freedom is 1984. Mesh has been generated with triangular elements, having a geometric side of 0.00005 (mm) for vessel and cell. We exploited a FEM implementation utilizing a time-dependent direct linear solver with parallel calculation [16].

Subsequently, we present final simulations in order to stress and strain results.

5. Results

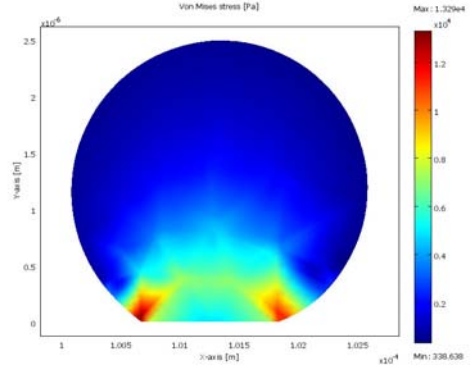


Figure 7. Example map of the Von Mises stress in a red blood cell.

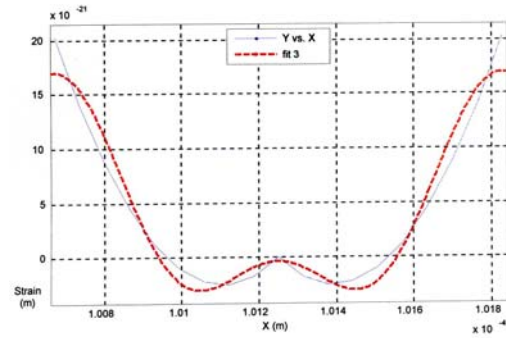


Figure 8. The non-monotone deformation law.

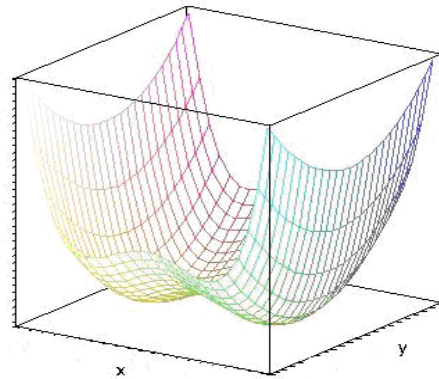


Figure 9. 3-D view of non-monotone deformation law.

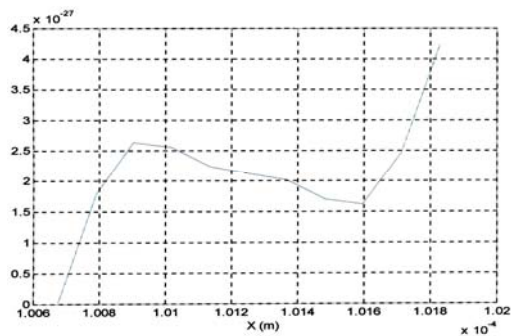


Figure 10. The complementary deformation density as integral of the deformation function.

6. Conclusions

The Simulated results were highly reliable, so our FEA package was very successfully simulating fluid–structure interaction in the human blood vessel. Our interest was to point out the concentration or inhomogeneity of the deformation on the contact area cell-wall. This particular result open the way to simulate the adhesion-detachment problem through more sophisticated model (i.e. functional analysis tools) such that microstructural characterization can be emphasized.

Results can be exploited in order to estimate the kind of human cell starting from signals obtained by computer simulations. Stress FEM maps have been used to train the Artificial Neural Network-based classifier. The authors are actually engaged in this direction.

7. References

1. B. Fabry, G.-N. Maksym, J.-P. Butler, M. Glogauer, D. Navajas, N.-A. Taback, E.-J. Millet, J.-J. Fredberg, Time scale and other invariants of integrative mechanical behavior in living cells, *Physical Review*, **68**, 0419141-04191418 (2003)
2. N. Mefti, B. Haussy, J.-F. Ganghoffer, Mechanical modeling of the rolling phenomenon at the cell scale, *International Journal of Solids and Structures*, **43**, 7378–7392 (2005).
3. P. Bongrand, A.-M. Benoliel, Adh sion cellulaire, *RSTD 44*, 167–178 (1999).
4. C.-C. Roberts, D.-A. Lauffenburger, J.-A. Quion, Receptor-mediated cell attachment and detachment kinetics: probabilistic model and analysis, *J. Biophys.*, **58**, 841–856 (1990).

5. P. Bongrand, Ligand–receptor interactions, *Rep. Prog. Phys.*, **62**, 921–968 (1982).
6. P. Villaggio, *Mathematical models for Elastic Structures*, Cambridge University Press, Cambridge (1997)
7. M.-J. Leitman, P. Villaggio, The Dynamics of Detaching Rigid Body, *Meccanica*, **38**, 595-609 (2003)
8. FEMLAB User's guide, Version 3.1: 474-490, COMSOL (2004)
9. J.-N. Reddy, *An Introduction to the Finite Element Method*, McGraw-Hill (1984)
10. O.-C. Zinkiewicz, K. Morgan, *Finite Element and Approximation*, John Wiley and Sons (1983)
11. N.-A. N'Dri, W. Shy, R. Tran-Son-Tay, Computational modeling of cell adhesion and movement using a continuum-kinetics approach, *Biophys. J.*, **85(4)**, 2273–2286 (2003)
12. D. Cheng, X-X. Lei, Biomechanics of cell rolling: shear flow, cell-surface adhesion, and cell deformability, *Journal of Biomechanics*, **33**, 35-43 (2000)
13. V. Nassehi, *Practical Aspects of Finite Element Modelling of Polymer Processing*, John Wiley and Sons, Chichester (2002)
14. F. Diacu, *An Introduction to Differential Equations*, Freeman and Company (2000)
15. I.-D. Huntley, R.-M. Johnson, *Linear and Nonlinear Differential Equations*, Ellis Horwood Ltd (1983)
16. R. Glowinski, T.-W. Pan, T.-I. Hesla, D.-D. Joseph, A distributed lagrange multiplier/fictitious domain method for particulate flows, *Int. J. Multiphase Flows*, **25**, 201–233 (1998)
17. B. Alberts, D. Bray, J. Lewis, M. Raff, K. Roberts, J.-D. Watson, *Molecular biology of the cell*, 3rd edn. Garland Science, Oxford (1994)

8. Acknowledgements

Many thanks to doctor and scientists of Transplant Regional Center of Stem Cells and Cellular Therapy, "A. Neri", Reggio Calabria, Italy, for the availability and for medical support useful to write this paper.

Many thanks also to researcher Buonsanti Michele, professor of mechanical engineering materials at the University "Mediterranea" of Reggio Calabria, Faculty of Engineering - MECMAT Department, for his support about mechanical aspects in human cells analysis.